Quantification of Bone Mineral Density in Human Cortical Bone by Solid State 31P MRI at 7 T

Alan C Seifert[1], Chamith S Rajapakse[1], Mahdieh Bashoor-Zadeh[1], Cheng Li[1], Yusuf A Bhagat[1], Alexander C Wright[1], Babette Zemel[2], Antonios Zavaliangos[3], and Felix W Wehrli[1]

[1]*Department of Radiology, University of Pennsylvania, Philadelphia, PA, United States,* [2]*Division of GI, Hepatology, and Nutrition, Children's Hospital of Philadelphia, Philadelphia, PA, United States,* [3]*Department of Materials Science and Engineering, Drexel University, Philadelphia, PA, United States*

Introduction: Phosphorus, whose only isotope, ^{31}P, has spin I=½, is a major component of bone mineral [1]. It has been shown that solid-state ^{31}P MRI has the potential to quantify bone mineral density [2-4], which, in combination with bone matrix density measured by solid-state ^{1}H MRI, can yield a measurement of true bone mineralization. Imaging of bone mineral phosphorus is made difficult by its extremely short T_2* (119.1 ± 0.4 μs) and long T_1 (66.0 ± 0.8 s) relaxation times [5], leading to substantial point spread function blurring, poor SNR, and long scan times. Using a zero echo-time (ZTE) pulse sequence to scan human cortical bone specimens from donors of different ages, we here show evidence that ex vivo quantitative solid-state ^{31}P MRI can identify age-related bone loss.

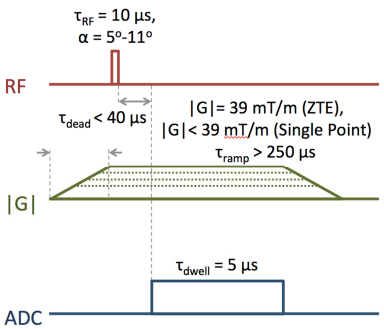

Figure 1: ZTE-PETRA imaging pulse sequence

Methods:

Specimens: Three whole-section bone specimens, each 36 mm long, were cut from tibiae obtained from female human donors (27, 53, and 83 years old, subsequently referred to as 27F, 53F, and 83F) at the location of maximum cortical thickness (a site corresponding to 38% of tibial length, measured from the medial malleolus). The bone specimens were sealed in plastic tubes with phosphate-buffered saline (having ^{31}P concentration of approximately 12 mM, orders of magnitude lower than in bone) and stabilized with PVC pipe at either end. Two intensity reference samples, constructed of hydroxyapatite powder inside sealed plastic drinking straws, were attached to the outside of the tubes before scanning.

Hardware: 7T whole-body MRI scanner (Siemens Magnetom, Erlangen, Germany) with 40 mT/m gradients. RF excitation and reception was performed using a custom solenoid coil 4.5 cm in diameter and 8 cm in length. Transmit/receive switching dead time was 50 μs.

Imaging and Reconstruction: Specimens were imaged using a 3-D radial zero echo-time (ZTE) pulse sequence with PETRA [6] (Fig. 1), which uses single-point acquisitions on a Cartesian grid within a central sphere of k-space to recover data lost during receiver dead time. Pulse sequence parameters are: TR = 250 ms, TE = 50 μs, flip angle = 5.0 degrees, |G| = 37.4 mT/m, dwell time = 5 μs, 128 points per readout, FOV = 310 mm isotropic, matrix size = 256x256x256, voxel resolution = 1.21 mm isotropic, PETRA radius = 10 points. K-space data were density-compensated by weighting each point by the 'volume' of k-space it occupies. The radial k-space data were mapped onto a Cartesian coordinate system, and then Fourier transformed. Each specimen was also imaged with peripheral quantitative computed tomography (pQCT, Orthometrix Stratec XCT2000, White Plains, NY) with a spatial resolution of 0.4x0.4x2.3 mm^3 in a single slice to obtain cortical bone mineral density, and with micro-computed tomography (μCT, Bruker, Kontich, Belgium) with a voxel size of (9 μm)^3 to measure bone tissue volume (total volume minus pore volume) and porosity (pore volume divided by total volume) by segmentation on a single slice.

Quantification: In each ^{31}P MR image, a volume of interest was defined inside each of the two intensity reference samples per image, and intensity in the entire image was normalized to the mean signal intensity within these two volumes of interest. The bone was segmented by thresholding at the average intensity of the reference samples and manually excluding the reference samples. Two ^{31}P MRI density measurements were recorded: apparent density, which is the total ^{31}P signal within the segmented bone divided by the apparent volume of bone tissue (including pores), and true density, which is the total ^{31}P signal divided by the true volume of bone tissue (excluding pores) measured by μCT. Apparent density, therefore, overestimates bone volume due to lack of sufficient spatial resolution and the resulting inability to resolve pore spaces and precise bone borders, while true density utilizes a more accurate measurement of bone tissue volume. Both pQCT bone mineral density and apparent ^{31}P MRI density measurements were also normalized by the volume fraction of mineralized bone tissue (excluding pore spaces) within the bone specimens, i.e. 100% - porosity.

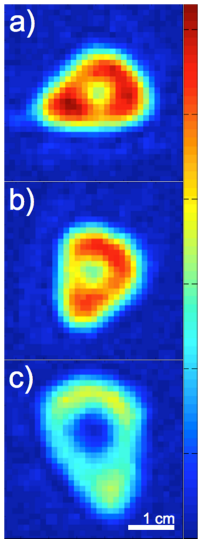

Figure 2: 31P density maps of a) 27 y/o, b) 53 y/o, and c) 83 y/o females, mutually normalized.

Results: Bones 27F, 53F, and 83F have apparent ^{31}P MRI densities of 1.08, 1.02, and 0.77 times the mean intensity within the two reference samples. For comparison, these bones have pQCT-derived mineral densities of 1245, 1242, and 1030 mg/cc, respectively. After correction for porosity, pQCT measurements in all three specimens are more consistent (1293, 1302, and 1274 mg/cc), while the corrected apparent ^{31}P MRI density of 0.95 in bone 83F is still noticeably lower relative to bones from the younger donors (1.12 and 1.07, respectively). True ^{31}P MRI densities in bones 53F and 83F are similar (1.02 and 1.03, respectively), while density in bone 27F is higher at 1.19.

Age	pQCT Density (mg/cc)	Bulk ^{31}P MRI Density (ArbU/mm^3)	μCT Volume Fraction (%)	Porosity-Corrected pQCT Density (mg/cc)	Porosity-Corrected Bulk ^{31}P MRI Density (ArbU/mm^3)	True ^{31}P MRI Density (ArbU/mm^3)
27	1245	1.08	96.30	1293	1.12	1.19
53	1242	1.02	95.38	1302	1.07	1.02
83	1030	0.77	80.88	1274	0.95	1.03

Table 1: Apparent and corrected pQCT mineral and ^{31}P MRI-based densities

Discussion and Conclusions: Osteoporosis, which is common in post-menopausal women, results in loss of bone tissue and enlargement of pores. Bone mineral density, measured with spatial resolution on a scale much larger than the pore architecture within cortical bone, generally decreases in age-related osteoporosis due to this expansion of the pore spaces [7]; this should therefore be denoted "apparent" density. In distinction, true bone mineral density (mineral per volume bone tissue, excluding pores) remains relatively constant. Due to the limited gradient strengths available in clinical whole-body scanners, point spread function (PSF) blurring in these images is severe, which may cause underestimation of even the macroscopic density in regions where the cortical thickness is less than the full width at half maximum of the point spread function (~3.9 mm at 7 T). Apparent ^{31}P MRI density was found to be 29% lower in bone 83F compared to 27F, but only 17% lower by pQCT. After correction for porosity, pQCT densities are similar in the three bones. Apparent ^{31}P MRI density in the relatively thin bone 83F still appears low after correction, but this is likely due to PSF blurring. True bone mineral density is similar in bones 53F and 83F, but is higher in 27F, possibly indicating a decreased level of mineralization in the bone from the oldest donor. Although quantification of phosphorus density was performed only relative to a reference sample, these preliminary data suggest potential of solid-state ^{31}P MRI to quantify absolute bone mineral density in vivo on a clinical scanner.

References: [1] Bringhurst FR In: Fauci AS, et al. Harrison's Principles of Internal Medicine. 17ed: McGraw-Hill Professional; 2008. [2] Wu Y, et al, PNAS 1999;1574-78. [3] Anumula S, et al, MRM 2006; 56:946-56. [4] Robson MD, et al, MRM 2004;51:888-92. [5] Seifert AC, ISMRM 2012; Abstract 1575. [6] Grodzki DM, et al., MRM 2012;67(2):510-518. [7] Zebaze R, et al., Bone 2009;44:S117-S118

Acknowledgements: NIH AR50068, F31 AG042289, K25 AR060283, Translational Bio-Imaging Center at the Penn Institute for Translational Medicine and Therapeutics.